AD-A244 256

CRREL

DTIC

S ELECTE **D**
JAN 0 3 1992
D

Energy Absorption of Graphite/Epoxy Plates Using Hopkinson Bar Impact

Piyush K. Dutta, David Hui and Magna R. Altamirano

October 1991

For conversion of SI metric units to U.S./British customary units of measurement consult ASTM Standard E380, Metric Practice Guide, published by the American Society for Testing and Materials, 1916 Race St., Philadelphia, Pa. 19103.

CRREL Report 91-20

Energy Absorption of Graphite/Epoxy Plates Using Hopkinson Bar Impact

Piyush K. Dutta, David Hui and Magna R. Altamirano

October 1991

92-00119

92 · · · 149

PREFACE

CONTENTS

ILLUSTRATIONS

Figure

Energy Absorption of Graphite/Epoxy Plates Using Hopkinson Bar Impact

PIYUSH K. DUTTA, DAVID HUI AND MAGNA R. ALTAMIRANO

INTRODUCTION

Most literature dealing with energy absorption in laminated composites describes the use of a dropweight or pendulum impact test apparatus. In these techniques, energy absorption is determined by subtracting the residual kinetic energy from the initial energy. Thus the effects of stress wave propagation, which is a source of damage initiation, cannot be examined using these testing techniques. Further, the laminate's energy absorption during the penetration process and the projectile's velocity, contact force, and duration of impact are difficult to measure. Hopkinson bar testing eliminates these restrictions and allows a thorough examination of the projectile impact process.

The effort described in this report involved an analytical and experimental study of energy absorption within graphite/epoxy plates impacted by a hemispherical-nosed impactor attached to a split Hopkinson bar test apparatus. The work is novel in that the plate's energy absorption was accurately measured using the recorded incident, reflected, and transmitted stress waves. The Hopkinson bar test apparatus allowed accurate determination of velocity, force, and energy absorption information during the entire impact duration. Thus the setup allowed "controlled" testing, capable of determining the energy absorption of impacted composite specimens. The only limitation was that the impactor was forced into the laminate at relatively low velocities.

MECHANICS OF WAVE PROPAGATION

The theoretical wave mechanics involved in the impact process are discussed based on elementary principles of unidirectional stress wave propagation. The duration of impact produced by the striker bar on the Hopkinson bar apparatus persists for a few hundred microseconds, and it takes a small but finite time for the effects of the impact force (stress wave) to enter the graphite epoxy test laminate at the opposite end of the bar. Upon entering the laminate, a portion of the incident stress wave is propagated into the transmitter bar and another portion is reflected back into the incident bar. Incident, reflected, and transmitted stress waves are measured by strain gauge instruments described elsewhere (Dutta et al. 1987).

In the current study, the laminate specimens consisted of 30 plies of AS4/3502 graphite epoxy with the following stacking sequence:

$$\left[\left(\pm 45/0_2 \right)_2 /90/\pm 45 /0_2/\pm 45 \right]_s$$

The indentor was driven into the laminate by the force of the incident bar's stress wave. Figure 1 shows a schematic of the Hopkinson bar, the impactor, and the laminate panel clamping assembly. Figure 2 is a photograph of the setup. The transmitter bar is free to slide forward or backward. As the striker hits the incident bar and drives the indentor into the laminate plate, the plate bends and behaves like a spring-mass system. Plate bending was recorded from strain gauges mounted on the rear face of the laminate.

The wave mechanics within this system was analyzed to determine the force–displacement relationship between the impactor and the composite laminate. Energy absorbed during the process was also determined as a function of time. The velocity, force, and energy absorbed were calculated from incident, reflected, and transmitted waveforms.

An impact of bar 1 (the striker bar) into bar 2 (the incident bar) produces a compressive force at interface A. According to elementary stress wave propagation
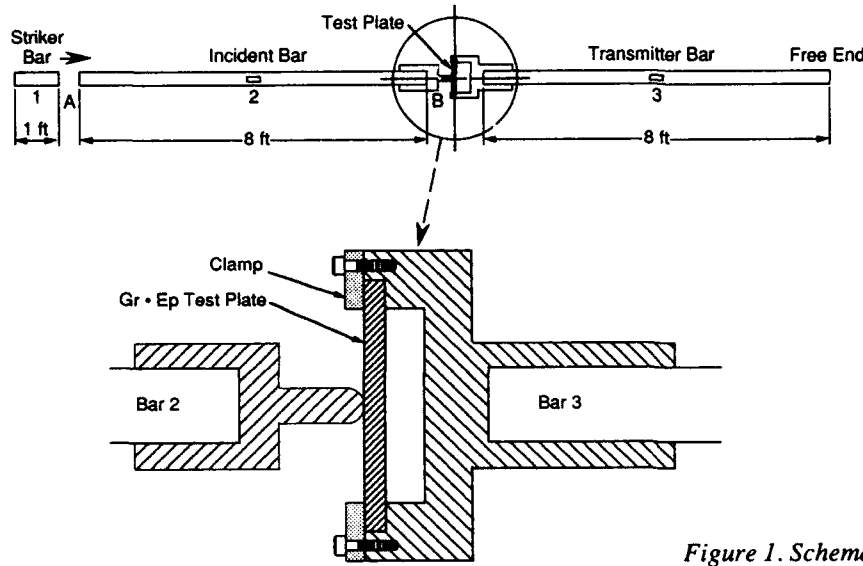
Figure 1. Schematic of the Hopkinson bar test setup.

theory (Kolsky 1963, Dutta et al. 1987), stress σ and force P generated by the impact are

$$\sigma = (\rho/g)\, c\, V \tag{1}$$

and

$$P = (A)(\rho/g)(cV) \tag{2}$$

where ρ is the density of the incident bar, g is the acceleration due to gravity, c is the speed of sound in the bar, V is the particle velocity in bar 2, and A is the cross-sectional area. The stress wave propagates along bar 2 to the opposite end where it encounters a discontinuity of its impedance (a product of density and stress wave velocity, ρc) at interface B. In the experimental setup, the impactor and laminate respond to this incoming stress pulse. As a result of the discontinuity, a portion of the stress pulse energy (E_I) is reflected (E_R) and a portion is transmitted (E_T) through the spring-mass system. Most of the remaining energy goes into the formation of plastic deformation of the plate. Some energy is also lost in overcoming frictional forces in various joints and through noise and vibration of the entire system. Net energy lost in the impact can be calculated by subtracting the energy of the transmitted and reflected waves from that of the incident wave:

$$E_A = E_I - E_R - E_T \tag{3}$$

The procedure for computing energy from the stress vs time waveform is given in Appendix A.

The force of penetration at any time t can be calculated more directly by considering the particle velocity in the following equation:

$$V = du/dt = \frac{\sigma}{\left(\dfrac{\rho}{g}\right)c} \tag{4}$$

where u is the axial displacement of the bar and is given by

$$u = \frac{1}{\left(\dfrac{\rho}{g}\right)c} \int_{t=0}^{t} \sigma(t)\, dt \tag{5}$$

Under the incident stress wave $\sigma_i(t)$, the penetrator end of bar 2 will be subjected to a displacement u_i given by

$$u_i = \frac{1}{\left(\dfrac{\rho}{g}\right)c} \int_{t=0}^{t} \sigma_i(t)\, dt \tag{6}$$

Due to the change of impedance, a portion of the stress wave is reflected, which produces a corresponding displacement of the indentor in the opposite direction; this displacement u_r is

2
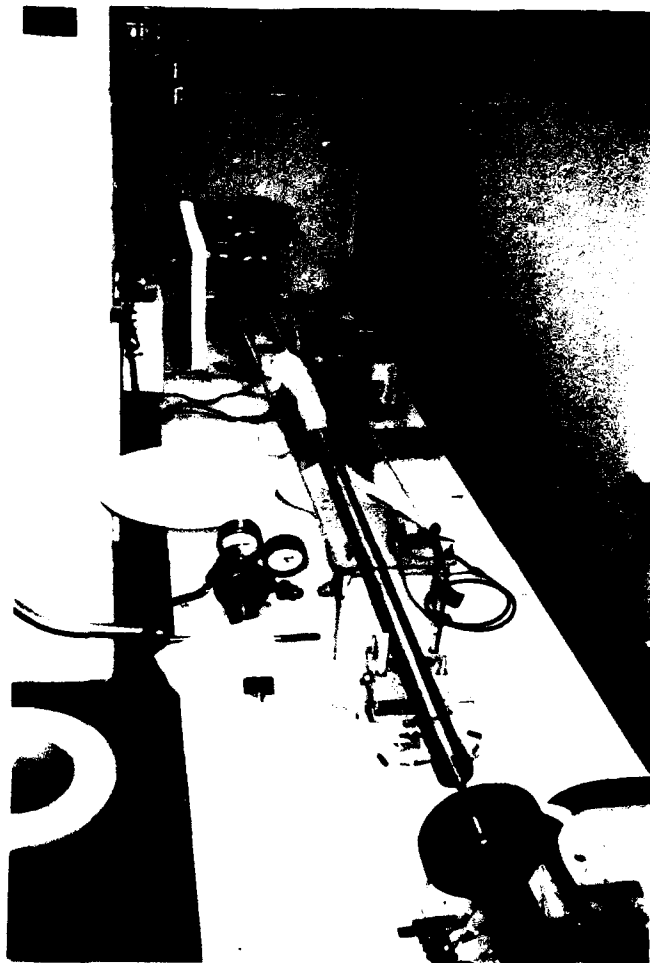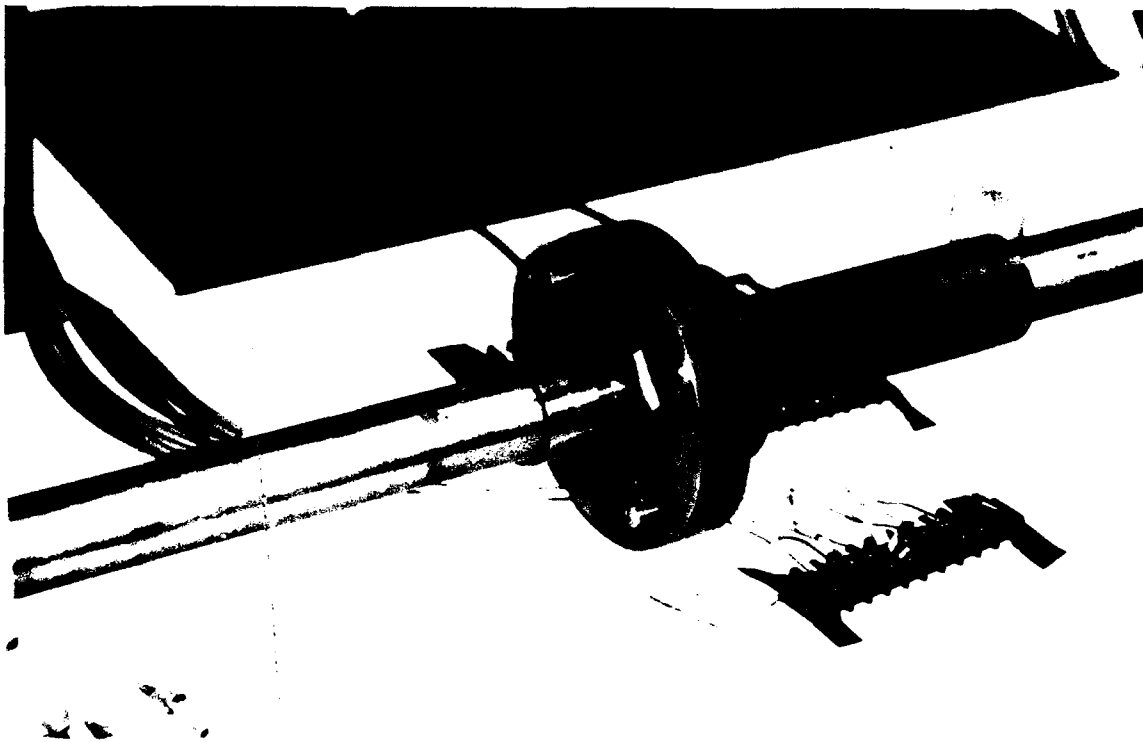
Figure 2. Photograph of the setup showing the hemispherical indentor.

3

$$u_r = \frac{1}{\left(\frac{\rho}{g}\right)c} \int_{t=0}^{t} \sigma_r(t)\, dt \qquad (7)$$

The resultant displacement u_t is given by

$$u_t(t) = \frac{1}{\left(\frac{\rho}{g}\right)c} \int_{t=0}^{t} \left[\sigma_i(t) - \sigma_r(t)\right] dt \qquad (8)$$

Force on the penetrator $[F(t)]$ is the algebraic sum of the incident force $A\sigma_i(t)$ and the reflected force $A\sigma_r(t)$:

$$F(t) = A \int_{t=0}^{t} \left\{\left[\sigma_i(t) + \sigma_r(t)\right]\right\} dt \qquad (9)$$

From eq 8 and 9, the force–displacement curve for the indentation can be plotted. The area under the curve will yield the energy absorbed as a function of time throughout the impact.

Energy absorbed by the graphite epoxy plate can be computed from the following energy balance equation (Greszczuk 1982, Shivakumar et al. 1984):

$$E_A = E_c + E_b + E_m + E_d + E_f \qquad (10)$$

where E_c = the energy expended in Hertzian contact indentation,

E_b = the energy due to plate bending,

E_m = the energy due to the stretching of the middle plate surface,

E_d = the energy due to permanent plate damage, and

E_f = the energy due to friction, heating, etc.

All of these energies are recoverable, except the damage and frictional energy. Plate damage may include any or all of the following modes of failure: matrix cracking, delamination, fiber breakage, and spalling.

The bending energy of a circular plate clamped along its edge under a concentrated load P is (Roark and Young 1975, Greszczuk 1982)

$$E_b = \left(P^2\right)\left(3a^2/2\right)\left(1 - v_r^2\right)\left(4\pi E_r h^2\right)^{-1} \qquad (11)$$

where a is the radius of the circular plate, h is the thickness of the plate, and E_r and v_r are the Young's modulus and Poisson's ratio, respectively, of the plate

material in the in-plane radial direction. Since the deflection was measured to be less than 20% of the laminate thickness, the membrane energy (E_m) was neglected.

Although Hertzian contact law was established for local static indentation of two elastic bodies, it is commonly applied to impact situations where permanent plastic deformations occur (Goldsmith 1960). The Hertzian contact energy of a spherical indentor with radius R impacting a flat plate is (Greszczuk 1982)

$$E_c = \left(P^{5/3}\right)\left(4/5\right)\left(3\pi/16\right)^{2/3}$$

$$\left[\left(k_1 + k_2\right)/\left(R/2\right)^{1/2}\right]^{2/3} \qquad (12)$$

where

$$k_1 = \left(1 - v_s^2\right)/\left(\pi E_s\right) \qquad (13)$$

$$k_2 = \left(1 - v_r^2\right)/\left(\pi E_z\right) \qquad (14)$$

where E_s and v_s are the Young's modulus and Poisson's ratio of the steel indentor, respectively, E_z is the laminate's modulus in the thickness direction, and v_r is the laminate's Poisson's ratio.

Assuming point contact between the indentor and plate, the deflection can be computed from the in-plane stress σ (Roark and Young 1975):

$$\sigma h^2/6 = \left[P/\left(4\pi\right)\right]\left(1 + v\right)$$

$$\left\{\ln\left[a/\left(0.325h\right)\right]\right\} \qquad (15)$$

Further, deflection y at the center of the circular plate due to a concentrated load P is

$$y = \left(Pa^2/\pi\right)\left(3/4\right)\left[\left(1 - v^2\right)/\left(Eh^3\right)\right] \qquad (16)$$

Measured strain can be converted to stress by multiplying the strain by the in-plane Young's modulus, so σ is a known quantity. Eliminating the applied load P from the above two equations, the deflection can be obtained in the form

$$y = \frac{a^2\sigma\left(1 - v\right)}{\left(2hE\right)\ln\left[a/\left(0.325h\right)\right]} \qquad (17)$$

Upon stress wave arrival, the indentor accelerates into the plate and creates a compressive stress wave that propagates through the thickness. Stress wave velocity
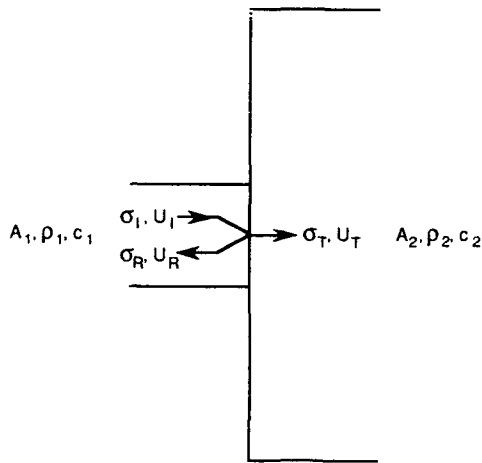
4

Figure 3. Stress pulse reflections and trans-
missions through the interface.

Figure 4. Interface velocity and force.

in the thickness direction of the plate is approximately (McMaster 1963)

$$c_z = \left[E_z / (\rho / g)^{1/2} f(v) \right] \tag{18}$$

$$f(v) = \left\{ (1 - v) / [(1 + v)(1 - 2v)] \right\}^{1/2} \tag{19}$$

where E_z is Young's modulus in the thickness direction and v is Poisson's ratio (for $n = 0.31, f(v) = 1.17732$).

For a quasi-isotropic graphite epoxy laminate, where $E_r = 51.16$ GPa (7.42 Msi), $E_z = 11.86$ GPa (1.72 Msi), and $\rho = 1522.4$ kg m^{-3} (0.055 lb-mass in.$^{-3}$), wave speed $c_z = 3.043$ km s^{-1} (0.1198 × 10^6 in. s^{-1}). This wave will propagate with speed c_z as a compressive wave and will eventually reflect off the rear (free) surface as a tensile wave with the same velocity. When the wave arrives at the rear surface, the plate moves away from the indentor

at velocity V_1 while the indentor continues to move into the plate with a velocity V_1 (see Fig. 3).

During the duration of the stress wave, three conditions are possible. First, when $V_2 < V_1$, the indentor accelerates into the plate (positive contact force) with a force vs time relationship as shown in Figure 4. Second, when $V_2 = V_1$, both the indentor and the plate move in the incident direction with no change in contact force. Third, when $V_2 > V_1$, loss of contact occurs between the indentor and plate, and a tensile force develops in the incident bar. Both the indentor and the plate move forward monotonically even though loss of contact occurs.

DISCUSSION OF RESULTS

Figure 5 is a graph of energy absorption vs displacement. The energy absorption of the plate (curve A) is
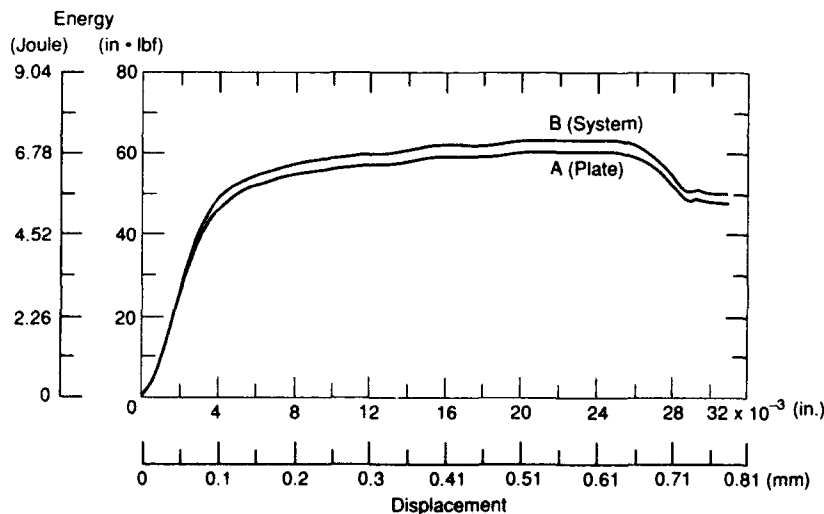
Figure 5. Impact energy absorption results.

5
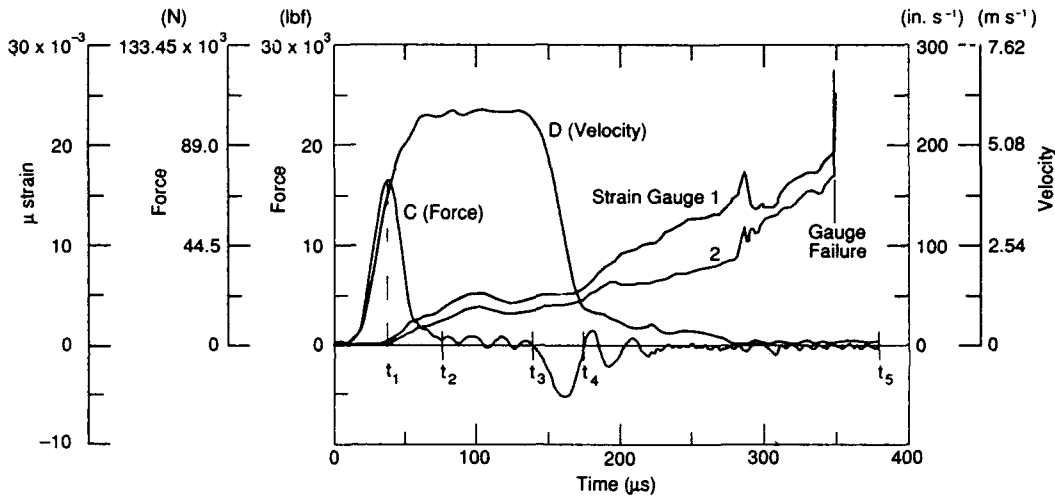
Figure 6. Results of force, velocity, and strain history measurements.

computed from the force vs displacement of the indentor. Energy absorbed in the system, consisting of the plate and clamping fixture shown in curve B, is computed from the incident, reflected, and transmitted waves. Appropriate formulae are given in Appendix A. The small difference between these two energy absorptions is the energy loss in the fixture (E_p).

Indentor force vs time (curve C of Figure 6) follows the model of Figure 4. There are five stages involved in the penetration process:

- In the initial loading stage ($0 < t < t_1$), the indentor accelerates into the plate, as can be seen from the increasing slope of the velocity trace (curve D).
- The second stage ($t_1 < t < t_2$) is the initial unloading stage where the indentor force decreases rapidly and the corresponding velocity increases at a slower rate. The drop in the indentor force is attributed to damage either in the contact region or near the rear surface due to a reflected tensile wave. The latter may cause the plate to move away from the indentor, thus reducing the contact force (which will be more evident in the next stage).
- The third stage is the constant velocity stage ($t_2 < t < t_3$) in which there is very little contact force. Referring to eq 9, note that at this stage $\sigma_I(t) = \sigma_R(t)$, indicating that there is no interfacial contact force.
- In the fourth stage ($t_3 < t < t_4$), the effects of stage 3 become more pronounced, and separation between the indentor and plate is possible. Similar loss of contact behavior has been reported by Wu and Springer (1988) and Sun and Chen (1985). At this stage, the applied incident stress amplitude begins to di-

minish but, because of the gap between the plate and the indentor, the indentor experiences a tensile force. (Note a reversal of the force direction.)

- The final stage ($t_4 < t < t_5$) is the vibration stage, during which the plate exerts an oscillating force on the indentor where contact may be lost and regained many times.

Figure 7 shows the cumulative energy absorption vs time. Energy absorbed increases rapidly with time in the first two stages and very slowly in the third stage. During the plate separation stage, a portion of the energy returns to the incident bar as the indentor accelerates into the free space in front of it. This energy is subtracted from the cumulative energy, so the energy curve dips at this stage. Energy absorbed in the final stage is constant and is the energy required to cause plate damage.

Figure 6 also shows data from two strain gauges mounted at two positions on the rear surface. Strain gauge 1 is mounted at the plate center and gauge 2 near the corner. The strain gauge data show that plate bending continually increases but remains small during the first four stages of impact. The increase becomes more pronounced in the final vibration stage and results in strain gauge failure near $t = t_5$.

Figure 8 shows the laminate's energy absorption E_A vs the maximum velocity of the indentor. The data follow the relationship

$$E_A = n\,V^{\,m} \tag{20}$$

where exponent m is found to be 2.55 for room temperature (21°C) and 4.53 for low temperature (−30°C). The value of the constant n for 21°C is 3.75×10^{-5} and for −30°C is 1.01×10^{-9}.

These data are currently considered a precursor to a

6
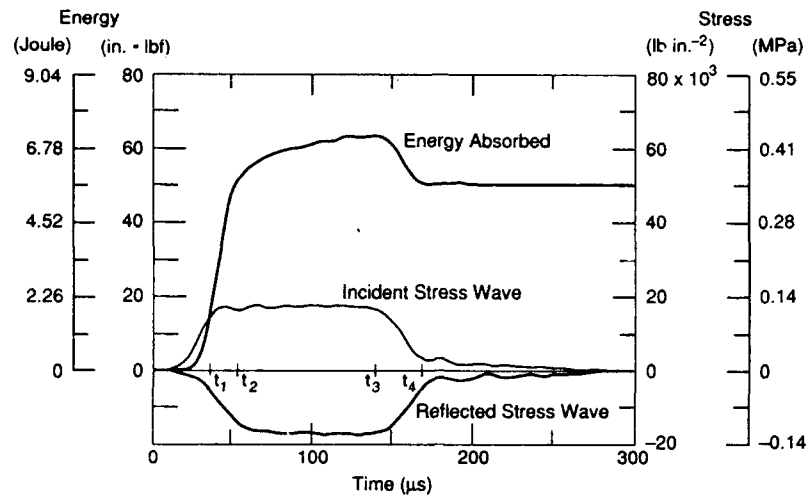
Figure 7. Bar stresses and energy absorption history.
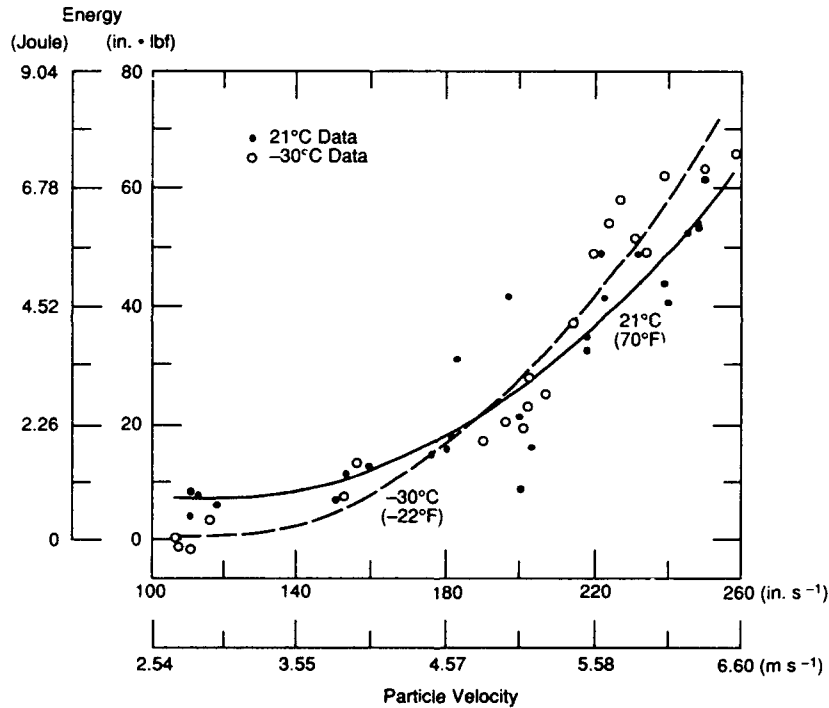
Figure 8. Influence of temperature and velocity on energy absorption.

detailed analysis of temperature's influence on the damage mechanisms associated with composite plate impact. It is well known that low temperature reduces the fracture toughness of most materials, but no extensive data are available for composites. In research performed by Nishijima and Okada (1982), cloth-reinforced epoxide resin composites were subjected to Charpy impact tests at room and liquid nitrogen temperatures. These tests demonstrated that a reduction in temperature causes a reduction in impact strength. Therefore, for a given

impact velocity more damage occurs at lower temperatures and more energy is absorbed. The experimental data in Figure 8 clearly show this trend after a transition velocity of about 4.8 m s^{-1} (190 in. s^{-1}). Above this velocity, more energy is absorbed by specimens held at low temperature. Below this transition velocity, the low temperature has an opposite effect, as discussed next.

Greszczuk (1982) and Shivakumar et al. (1985) have shown that in the low velocity range, among non-recoverable energies, the Hertzian contact force is the

7

Figure 9. Effect of temperature on Hertzian contact energy.

Figure 10. Energy loss as a function of impact energy (after Sjoblom et al. 1988).

most dominating energy absorption mechanism. From eq 12 this energy is a function of $(k_1 + k_2)^{2/3}$. Substituting $v_s = 0.3$ and $E_s = 206.9$ GPa (30×10^6 psi) for a steel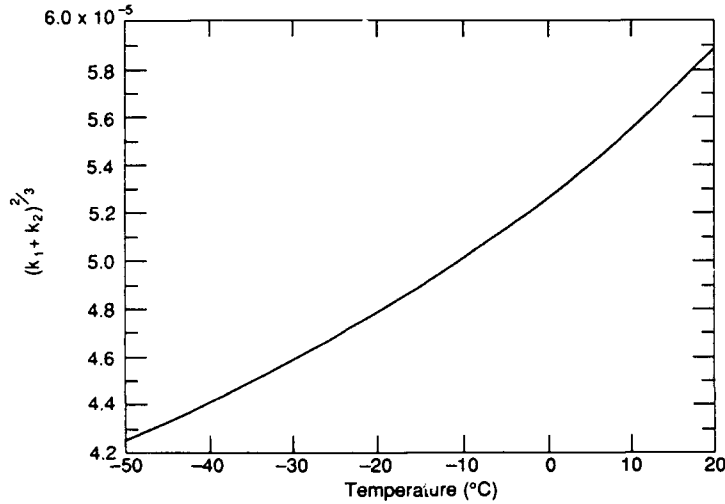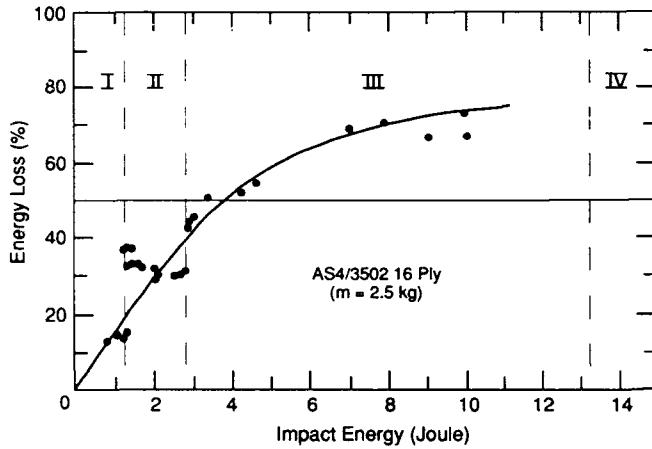 indentor into eq 13, $k_1 = 0.9.67 \times 10^{-9}$. Referring to eq 14, k_2 contains the term E_s (the Young's modulus of the composite plate in the thickness direction), which is influenced at low temperature by the change in elastic modulus E_m of the resin matrix. The empirical relation established by Dutta (1989) for matrix stiffening with lower temperature is

$$E_m(T) = E_m(T_0) - 2.9 \times 10^3 (T - T_0) \qquad (21)$$

where T_0 is the room temperature and T is the low temperature in °C. Applying the above relationship to the rule-of-mixtures equation (Tsai and Hahn 1980)

$$E = \frac{E_f E_m}{V_f E_m + V_m E_f} \qquad (22)$$

yields

$$E_z = \frac{E_f E_m(T)}{v_f(T) E_m(T) + v_m E_f} \qquad (23)$$

where v_m and v_f are the matrix and fiber volume ratios, and E_m and E_f are the matrix and fiber modulus of elasticity. (T) indicates the prevailing temperature of the matrix. Solving for E_z and setting $v_r = 0.31$, k_2 is determined via eq 14. Figure 9 shows a plot of $(k_1 + k_2)^{2/3}$ vs temperature. It is clear from this graph that as the temperature is reduced the value of E_c (the Hertzian contact energy, which is a direct function of $(k_1 + k_2)^{2/3}$) decreases. The experimental results in Figure 8 confirm this.

In a separate ballistic experiment involving the penetration of identically configured 30-ply graphite epoxy laminates by 12.7 mm (0.5 in.) spheres, Mayer and Altamirano* observed energy absorption E_a in the form

---

* Personal communication (1990) from A. Mayer, Air Force Wright Laboratories, Dayton, Ohio.
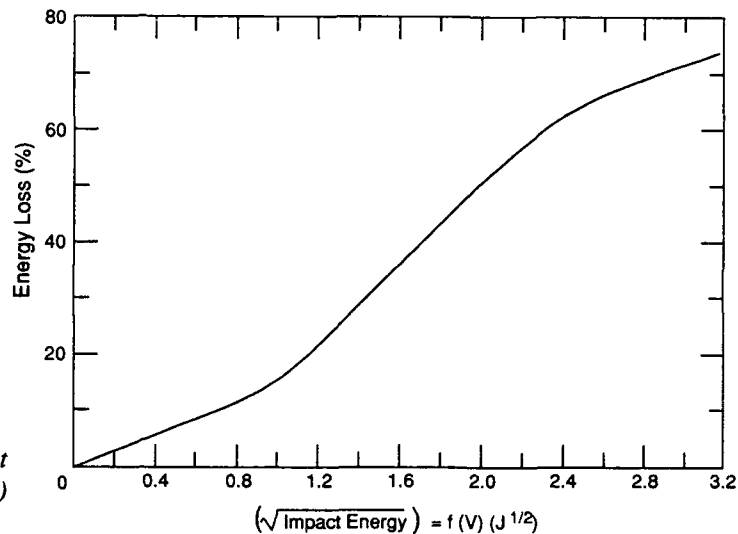
8

Figure 11. Energy loss as a function of impact velocity as obtained from Sjoblom et al. (1988) data.

$$E_a = C_0 V^{1.489} \tag{24}$$

where V is the impact velocity and C_0 is a constant. Experimental velocities ranged from 500 to 1500 m s^{-1} (1600–4900 ft s^{-1}). Comparing the exponents of V from the three series of experiments—1.489 from the ballistic tests, 2.55 from the Hopkinson bar room-temperature tests, and 4.53 from the Hopkinson bar low-temperature tests—it is clear that the damage mechanisms and energy partitioning are different at higher velocities than under Hopkinson bar low-velocity impact. The lower value of the exponent suggests a failure mechanism that progressively requires less energy as the velocity is increased. This trend was also validated by Sjoblom et al. (1988) (Fig. 10). The solid line in this figure shows that energy loss is a function of V^2. A reconstruction of the energy loss vs velocity (Fig. 11) clearly shows a decrease in the energy absorption rate at higher velocities.

CONCLUSIONS

The energy absorption of laminated plates under normal impact generated by a Hopkinson bar apparatus was examined. Using wave propagation theory, the energy absorption agrees with theoretical predictions. The force, velocity, and energy were recorded throughout the impact event, which encompassed several hundred microseconds. The experimental procedure provided a controlled condition enabling the full analysis of events during this period. Loss of contact between the impactor and laminate occurred frequently during the impact process due to stress waves in the plate reflecting back and forth through the thickness. The energy balance equation provides a powerful tool for analyzing the energy available to cause laminate damage.

Low temperatures influence the energy absorption characteristics and control the damage mechanisms. Existence of a transition velocity was observed; above this velocity energy absorption from an impact is higher than at room temperature. At low temperature, reduced impact strength causes a larger volume of damage. Below the transition velocity (at low temperatures) the laminate absorbs less energy, which can be approximated by Hertzian contact theory.

When comparing data generated via the Hopkinson bar apparatus to data obtained via high velocity ballistic impact, the failure mechanism is seen to be a function of impact velocity. As the impact velocity increases, the fracture requires less energy.

LITERATURE CITED

Dutta, P.K. (1989) A theory of strength degradation of unidirectional fiber composites at low temperature. *Proceedings of the Industry-University Advanc ed Materials Conference,* Advanced Materials Institute, Colorado School of Mines, March 6–9 (F.W. Smith, Ed.), p. 647–662.

Dutta, P.K., D. Farrell and J. Kalafut (1987) The CRREL Hopkinson bar apparatus. USA Cold Regions Research and Engineering Laboratory, CRREL Special Report 87-24.

Goldsmith, W. (1960) *Impact.* London: Edward Arnold (Publishers), Ltd., p. 82–144.

Greszczuk, L.B. (1982) Damage in composite materials due to low velocity impact. Chapter 3 in *Impact Dynamics* (J.A. Zukas et al., Ed.). New York: John Wiley and Sons, p. 55–94.

Kolsky, H. (1963) *Stress Waves in Solids.* New York: Dover Publications.

McMaster, R.C. (1963) *Nondestructive Testing Handbook*. New York: Ronald Press Co., p. 43.9–10.

Nishijima, S. and T. Okada (1982) Charpy impact test of cloth reinforced epoxide resin at low temperature. In *Nonmetallic Materials and Composites at Low Temperatures* (G. Hartwig and D. Evans, Ed.). New York: Plenum Press, p. 259–275.

Roark, R.J. and W.C. Young (1975) *Formulas for Stress and Strain*. New York: McGraw-Hill Book Co., p. 332–367.

Shivakumar, K.N., W. Elber and W. Illg (1985) Prediction of impact force and duration due to low-velocity impact on circular composite laminates. *ASME Journal of Applied Mechanics*, 55: 674–680.

Sjoblom, P.O., T.J. Hartness and T.M. Cordell (1988) On low-velocity impact testing of composite materials. *Journal of Composite Materials*, 22: 30–52.

Sun, C.T. and J.K. Chen (1985) On the impact of initially stressed composite laminates. *Journal of Composite Materials*, 19: 490–504.

Tsai, S.W. and H.T. Hahn (1980) *Introduction to Composite Materials*. Lancaster, Pennsylvania: Technomic Publishing Co., p. 389.

Wu, H.Y.T. and G.S. Springer (1988) Impact induced stresses, strains and delaminations in composite plates. *Journal of Composite Materials*, 22: 533–560.

APPENDIX A: WAVE PROPAGATION IN A HOPKINSON BAR APPARATUS

The incident, reflected, and transmitted energy are denoted by E_I, E_R, and E_T respectively. The governing equations for stress $\sigma(t)$, velocity $V(t)$, and displacement $u(t)$ are

$$\sigma(t) = (\rho)(c/g) V(t) \tag{A1}$$

$$V(t) = du/dt \tag{A2}$$

$$u(t) = (c/E) \int_{t=0}^{t} \sigma(t) \, dt \tag{A3}$$

where E = Young's modulus,
    t = time,
    ρ = density,
    $V(t)$ = velocity,
    c = the wave speed in the material, and
    g = the acceleration due to gravity.

Further, the energy of the wave in a one-dimensional bar is

$$E = \frac{Ac}{E} \int_{t=0}^{t} \sigma^2(t) \, dt \tag{A4}$$

where A is the cross-sectional area of the circular Hopkinson bar. Displacement of the indentor $u_I(t)$ can be obtained from the incident, reflected, and transmitted stresses ($\sigma_I(t)$, $\sigma_R(t)$, and $\sigma_T(t)$, respectively):

$$u_I(t) = (c/E) \int_{t=0}^{t} \left[\sigma_I(t) - \sigma_R(t) - \sigma_T(t) \right] dt \tag{A5}$$

The force on the indentor is

$$F(t) = (A) \left[\sigma_I(t) + \sigma_R(t) \right] \tag{A6}$$

Energy produced by the indentor (E_p) can be computed from an integration of the product of force and displacement over the duration of the wave:

$$E_p = (Ac/E) \int_{t=0}^{t} \left\{ \left[\sigma_I(t) + \sigma_R(t) \right] - \left[\sigma_I(t) - \sigma_R(t) - \sigma_T(t) \right] \right\} dt \tag{A7}$$

The energy of the incident, reflected, and transmitted waves can then be computed from

$$(E_I, E_R, E_T) = (Ac/E) \int_{t=0}^{t} \left[\sigma_I(t)^2, \sigma_R(t)^2, \sigma_T(t)^2 \right] dt \tag{A8}$$

11

The total energy absorbed within the system (i.e. that absorbed during damage generation and minor losses within the fixture) is

$$E_A = E_I - (E_R, E_T),$$ (A9)

which can be rewritten as

$$E_A = (Ac/E) \int_{t=0}^{t} \left\{ \sigma_I(t)^2 - \left[\sigma_R(t)^2 + \sigma_T(t)^2 \right] \right\} dt$$ (A10)

The Hopkinson bars used in this test series were steel with the following parameters:

$A = 1140 \text{ mm}^2 (1.7675 \text{ in.}^2)$
$c = 5017 \text{ m s}^{-1} (197531 \text{ in. s}^{-1})$
$E = 193.05 \text{ GPa} (28 \times 10^6 \text{ psi})$

so that $Ac/E = 0.02963 \text{ m}^3 \text{ GPa}^{-1} \text{ s}^{-1} (0.012467 \text{ in.}^5 \text{ lb}^{-1} \text{ s}^{-1})$.

REPORT DOCUMENTATION PAGE

Public reporting burden for this collection of information is estimated to average 1 hour per response, including the time for reviewing instructions, searching existing data sources, gathering and maintaining the data needed, and completing and reviewing the collection of information. Send comments regarding this burden estimate or any other aspect of this collection of information, including suggestion for reducing this burden, to Washington Headquarters Services, Directorate for Information Operations and Reports, 1215 Jefferson Davis Highway, Suite 1204, Arlington, VA 22202-4302, and to the Office of Management and Budget, Paperwork Reduction Project (0704-0188), Washington, DC 20503.

1. AGENCY USE ONLY (Leave blank)	2. REPORT DATE October 1991	3. REPORT TYPE AND DATES COVERED

4. TITLE AND SUBTITLE

Energy Absorption of Graphite/Epoxy Plates Using Hopkinson Bar Impact

6. AUTHORS

Piyush K. Dutta, David Hui and Magna R. Altamirano

5. FUNDING NUMBERS

PE: 6.27.84A
PR: 4A762784AT42
TA: SS
WU: 019
        and
MIPR FY1456-90-N0066

7. PERFORMING ORGANIZATION NAME(S) AND ADDRESS(ES)

U.S. Army Cold Regions Research and Engineering Laboratory
72 Lyme Road
Hanover, New Hampshire 03755-1290

8. PERFORMING ORGANIZATION REPORT NUMBER

CRREL Report 91-20

9. SPONSORING/MONITORING AGENCY NAME(S) AND ADDRESS(ES)

Office of the Chief of Engineers   U.S. Air Force Flight Dynamics Laboratory
Washington, D.C. 20314-1000   Wright Patterson AFB, Ohio

10. SPONSORING/MONITORING AGENCY REPORT NUMBER

11. SUPPLEMENTARY NOTES

12a. DISTRIBUTION/AVAILABILITY STATEMENT

Approved for public release; distribution is unlimited.

Available from NTIS, Springfield, Virginia 22161

12b. DISTRIBUTION CODE

13. ABSTRACT (Maximum 200 words)

This work summarizes the analytical and experimental study on the energy absorption of quasi-isotropic graphite/epoxy composite plates due to the impacting hemispherical penetrator in a Hopkinson bar apparatus. The mechanics of stress wave propagation through the bar and the composite laminate plate are discussed to predict the phenomenological process involved. The experimental data provided the results in terms of force, velocity, and energy of impact at all times during the penetration process occurring in microseconds. It has been concluded that loss of contact occurs frequently during the penetration process due to the stress wave reflections back and forth in the thickness direction. The damage process seemed to be both velocity and temperature dependent. Below a certain transition velocity the laminate absorbs less energy at low temperature than at high temperature. The reverse is true above this transition velocity. The mechanism of failure tends to change with impact velocity in such a way that progressively less energy is absorbed at higher velocities.

14. SUBJECT TERMS

Advanced composites	Composites	Fiber composites	Impact	Stress wave
Cold	Damage	Graphite/epoxy	Low temperature	

15. NUMBER OF PAGES
18

16. PRICE CODE

17. SECURITY CLASSIFICATION OF REPORT	18. SECURITY CLASSIFICATION OF THIS PAGE	19. SECURITY CLASSIFICATION OF ABSTRACT	20. LIMITATION OF ABSTRACT
UNCLASSIFIED	UNCLASSIFIED	UNCLASSIFIED	UL

* U.S. GOVERNMENT PRINTING OFFICE: 1991-600-063/42-39 REGION 1